JOURNAL OF MATERIALS SCIENCE **35** (2000) 2229–2233

Thermal stability and mechanical performance of multiply heat-treated α-sialon ceramics densified with rare earth oxides

Q. LIU, L. GAO, D. S. YAN
The State Key Lab of High Performance Ceramics and Superfine Microstructure, Shanghai Institute of Ceramics, 1295 Dingxi Road, Shanghai 200050, People's Republic of China
E-mail: qianliu@sic.ac.cn

D. P. THOMPSON
Materials Division, Department of Mechanical, Materials and Manufacturing, University of Newcastle upon Tyne, NE1 7RU, United Kingdom

Typical α-sialon starting compositions, of formula $Ln_{0.33}Si_{9.3}Al_{2.7}O_{1.7}N_{14.3}$, were densified by hot-pressing using Ln_2O_3 as sintering additives, where Ln = Nd, Dy, and Yb. The as-sintered materials were heat-treated at 1450°C for 96 hours and then re-sintered at 1800°C for 1 hour to observe the overlapping effects of both Ln_2O_3 and multiple heat-treatment on thermal stability of the Ln-α-sialon phase and also the change in microstructure. The kinds of grain boundary phases which occurred also affected the results. The hardness, fracture toughness and flexural strength of the materials were evaluated using indentation and three-point bending tests, respectively. Mechanical tests and detailed microstructural analysis have led to the conclusion that a multiple-mechanism is involved, with debonding, crack deflection, crack bridging, and elongated grain pull-out all making a significant contribution towards improving the fracture toughness. Nd-containing specimens were tough with a highest indentation fracture toughness K_{1C} of 7.0 MPa $m^{1/2}$. In contrast, Dy- and Yb-containing specimens were hard and brittle with a highest Vickers hardness H_{V10} of 18.0 GPa. All re-sintered specimens underwent $\beta \rightarrow \alpha$ transformation to some degree, leading to a degradation of mechanical properties as a consequence.

1. Introduction

Sialons, solid solutions of aluminum and oxygen in silicon nitride, have been widely studied for several decades as engineering ceramics, either in the α- or β-forms. From a preparative point of view, it is much easier to tailor the microstructure and properties of an α-sialon material, because of the wide solid solution range available for composition selection and also because of the possibility of $\alpha \rightarrow \beta$ phase transformation. Concerning the mechanism of toughening as well as strengthening, *in-situ* reinforcement via elongated sialon grains has proved an effective intrinsic approach (by debonding, pull-out, crack bridging, and crack deflection) and has been suggested as a preferable alternative to extrinsic reinforcement (e.g. using platelets and whiskers), since it improves production economics, thermal stability, and environmental safety.

Isostructural with Si_3N_4, sialon has two forms, α-sialon (α') and β-sialon (β'). The general formula of α-sialon is represented as $M_xSi_{12-m-n}Al_{m+n}O_nN_{16-n}$, where $x < 2$ and M cations Li, Mg, Ca, Y, La, and most rare earth ions (Ln) are incorporated into interstitial sites in the α' network. However, the α' structure can accommodate these M cations when available from liquid phase sintering additives, leaving a minimal compositional residue at grain boundaries in the final material, which is an important consideration in the development of fully dense sialon materials for use at elevated temperatures. On the other hand, the α' phase usually forms as equiaxed grains which are therefore of low toughness due to the lack of the conventional pull-out toughening mechanism provided by elongated grains. However, α' ceramics show unique hardness due to their intrinsically higher hardness compared with β' phase. β-sialon, of formula $Si_{6-z}Al_zO_zN_{8-z}$, is tougher by self-reinforcement because the final microstructure contains elongated grains. An additional important variable is that at the temperatures used to sinter and heat-treat sialon ceramics, rare earth α-sialons are unstable and transform to β', thereby modifying the microstructure and hence the mechanical behaviour. Besides, heat treatment is an effective method for minimizing the grain boundary glass in nitrogen ceramics by converting it into refractory crystalline phase(s), thus improving the high temperature properties [1–6]. The present work is based on the idea of designing a series

of rare earth oxide-densified monolithic sialon ceramics with adequate thermal stability and enhancement not only of the hardness but also of the toughness by building up a mosaic assemblage of equiaxed and elongated grains by controlled in-situ $\alpha \Leftrightarrow \beta$ sialon transformation. Previous studies have shown that $\alpha' \rightarrow \beta'$ transformation proceeds at different rates when different rare earth oxide densification additives are used [7–10], leading to the formation of different microstructures. There are therefore many parameters (e.g. starting composition, sintering additives, sintering methods, schedule of heat-treatment, and environment) which can be adjusted for property optimization. The aim of this work has been to determine the effects of various rare earth oxide additives and to relate the extent of transformation by multiple heat-tretment to the modification of microstructure and the changes in mechanical properties.

For this purpose, light (Nd_2O_3), medium (Dy_2O_3), and heavy (Yb_2O_3) rare earth oxides were chosen as densifying additives to compare their effect on α' thermal stability. The hot-pressed materials were not only heat treated at 1450°C for 96 hours but also re-sintered at 1800°C for 1 hour to figure out the overlapping effects of the two heat processing on $\alpha' \rightarrow \beta'$ transformation. That is one area of newness in this research. The effect of different cation size sintering additives on the thermal stability, microstructural characteristics and hence mechanical performance (H_{V10}, K_{1c}, and σ_f) were evaluated.

2. Experimental procedure

The starting compositions were very similar and corresponded to compositions at the low-m α-sialon boundary of the type $Ln_{0.33}Si_{9.3}Al_{2.7}O_{1.7}N_{14.3}$, with Ln = Nd, Dy, and Yb. Sialon starting powders (i.e. Si_3N_4, Al_2O_3, AlN, and Ln_2O_3) were ball milled using Si_3N_4 balls in isopropanol for one day to prepare a suspension. The fresh suspension was processed by magnetic stirring, drying, and then sieving. The resulting powders were hot- pressed in BN-coated graphite dies at 1800°C for one hour at a pressure of 30 MPa. As-sintered samples were heat-treated in an alumina tube furnace in flowing nitrogen at 1450°C for 96 hours, and re-sintered in a carbon resistance furnace at 1800°C for 1 hour under a protective nitrogen atmosphere, and then the furnace was cooled at a rate of 50°C min^{-1} from 1800 to 1200°C to modify the microstructure and change the α'/β' ratio. Before being heat-treated and re-sintered, the specimens were embedded in micron-sized boron nitride powder in graphite crucibles. Densities of the samples were measured with a mercury displacement balance using Archimedes' principle. Phase identification was carried out by x-ray diffraction using a Hagg-Guinier focusing camera with Cu $K_{\alpha 1}$ radiation, and using the intensities of the (102) and (210) peaks of the α-sialon phase and the (101) and (210) peaks of the β-sialon phase for quantitative estimation of the α/β sialon ratio. The Vickers hardness as well as indentation fracture toughness were determined at room temperature by indentation using a Vickers diamond indenter and a load of 98 N for 10 minutes. The hardness and fracture toughness were evaluated according to the method of Evans andCharles [11]. The flexural strength of samples (30 × 3.5 × 2.5 mm) was measured at a constant cross-head speed of 0.2 mm/min using a three-point bending equipment (C100D-testing Machine, R. D. P.-Howden) with an outer span of 20 mm. The measured strength values were used to provide reference data because only 2–3 bars for each sample were available for testing due to the limitation of sample size. All samples for mechanical property measurements were ground and polished with diamond pastes of size 45 μm, 25 μm, 14 μm, 6 μm, and 1 μm. SEM microstructural studies were carried out using a HITACHI SEM (S-2400) instrument.

3. Results and discussion

3.1. Thermal stability and reversible $\alpha \Leftrightarrow \beta$ transformation of Ln-α-sialons

X-ray analysis of Ln-α' phase content in samples hot-pressed at 1800°C, heat-treated at 1450°C, and re-sintered at 1800°C is illustrated in Fig. 1. The levels of α' phase formation were quite different in the Nd-, Dy-, and Yb-system. Whereas the as-sintered samples, originally designed to give pure Nd-α', now contained some β' phase (about 30%), but the original Dy- and Yb-α' samples were still almost pure α' phase. The α-sialon stability was highly marked in the case of samples densified with higher atomic number rare earth oxides, and arises mainly because of the larger homogeneity range of the heavy rare earth α-sialon phase [12, 13]. This is also obviously apparent from SEM micrographs shown in Fig. 2. Fig. 2 shows the microstructural changes in Nd-containing samples before and after post-heat-treatment. Back-scattered electron micrographs give a sharp contrast between the various phases: β' grains without rare earth element are black and more elongated, whereas the α' grains accommodating rare earth cations are gray and more equiaxed, whilst Nd-rich crystalline or glassy phase is white.

To study the effects of temperature on the thermal stability of Ln-α-sialon in more detail, the hot-pressed samples were heat-treated at 1450°C for 96 h. The thermal stability of the α'phase was obviously dependent on the kind of additive, i. e. Nd_2O_3, Dy_2O_3, or Yb_2O_3.

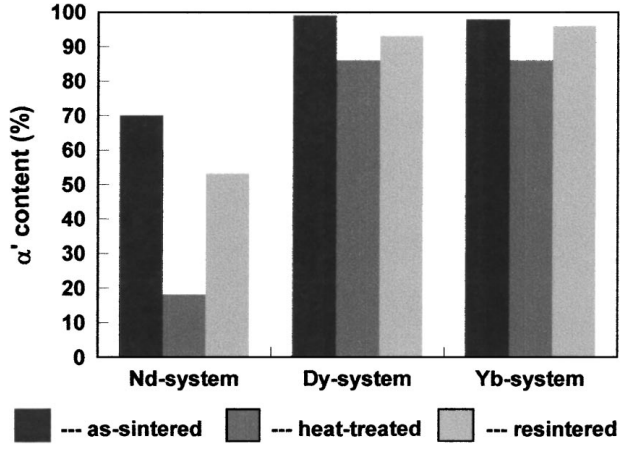

Figure 1 XRD analysis of α-sialon phase contents in Ln-added samples before and after post-heat-treatment.

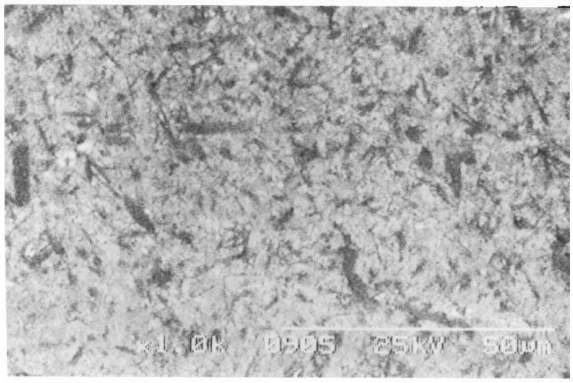

(a)

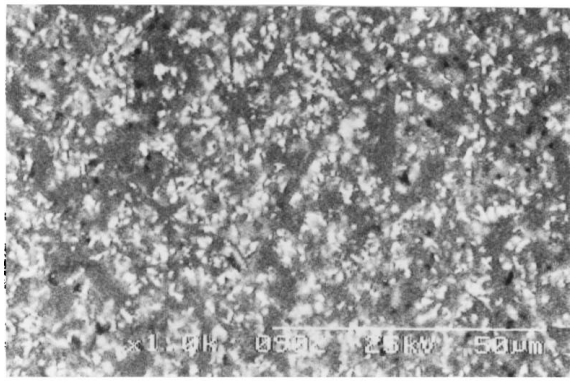

(b)

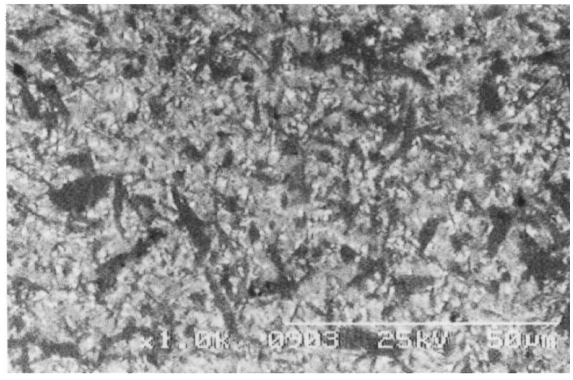

(c)

Figure 2 Backscattered SEM micrographs illustrating the microstructural changes in grain morphology and phase distribution in Nd-sialon before (a) and after heat-treatment (b) as well as resintering (c), in which β' grains are black, α' grains are grey and grain boundary phases are white.

In Nd-densified samples, the α-sialon was very unstable at 1450°C and transformed extensively to β' phase plus Nd-M′ (the $Nd_2Si_3O_3N_4$ melilite phase, but with some substitution of Si and N by Al and O) as the main grain boundary crystalline phase. In contrast, Dy- and Yb-densified samples both showed good stability of the α' phase at 1450°C with only a small amount of β' produced. The main crystalline grain boundary phase produced in these two cases was garnet ($Dy_3Al_5O_{12}$, $Yb_3Al_5O_{12}$). Concerning the mechanism of $\alpha' \rightarrow \beta'$ transformation, it has previously been concluded that this occurs at temperatures above 1350°C and is a reconstructive polymorphic transformation which is essentially chemically controlled via a solution-diffusion-precipitation route [14]. The transformation during 96 h at 1450°C for Nd-, Dy-, and Yb-samples proceeds according to the overall equation [15, 16]:

$$\text{Liquid} + \alpha' \rightarrow \beta' + \text{crystalline grain boundary phase} + \text{residual glass} \quad (1)$$

where the main crystalline grain boundary phase is melilite in the Nd-samples, and garnet in both Dy- and Yb-samples. The transformation occurred with elongated β' grains developing in the matrix and rare-earth elements being transferred via liquid phase from α' grains to crystalline grain boundary phases.

In addition, it was of interest to discover whether re-sintering had a significant overlapping effect on $\alpha' \rightarrow \beta'$ transformation and re-sintering of the heat-treated samples was therefore performed at 1800°C. In this case reverse $\beta' \rightarrow \alpha'$ transformation occurred and the α' phase content in all samples greatly increased, as seen in Fig. 1. This was most marked for the lower atomic number rare earth oxides, for example, the Nd_2O_3-densified sample, which contained 70% α' and 30% β' before heat treatment, and after heat treatment at 1450°C for 96 hours changed to 18%α'–82% β', greatly changed to 54%α'–46%β' after 1800°C re-sintering. A similar transformation tendency also occurred for Dy_2O_3- and Yb_2O_3-densified samples but to a lesser extent, with these samples showing nearly 100% α' before heat treatment, changed to 85% α'–15% β' after 1450°C heat treatment, and back to 95% α'–5% β' after 1800°C re-sintering. The microstructure of these samples also revealed the change in α'/β' ratio by the changes in grain morphology and the amounts of different phases including grain boundary phase, as shown in Fig. 3.

3.2. Mechanical behaviour

The densities of samples hot-pressed, heat-treated and re-sintered are summarized in Table I. All hot-pressed samples reached essentially full density. The density decreased after heat-treatment and re-sintering. The samples heat-treated at 1450°C for 96 hours in a BN powder bed exhibited weight losses of no more than 1.0% and this may be attributed to loss of SiO and nitrogen gas. The weight losses in the re-sintered samples were more serious even though a BN powder bed was used.

As mentioned above, all samples sintered at 1800°C gave quite different responses when heat-treated at 1450°C for 96 h. The main difference was that relatively small amounts of $\alpha' \rightarrow \beta'$ transformation occurred in the Dy- and Yb-samples, whereas in the Nd-samples much more $\alpha' \rightarrow \beta'$ transformation occurred; moreover the appearance of various grain boundary phases resulted in significant changes in microstructure, thus

TABLE I Densities (g/cm^3) of Ln-sialons as-sintered and post-heat-treated

	As-sintered	Heat-treated	Re-sintered
Nd-sialon	3.36	3.32	3.31
Dy-sialon	3.38	3.37	3.36
Yb-sialon	3.42	3.41	3.39

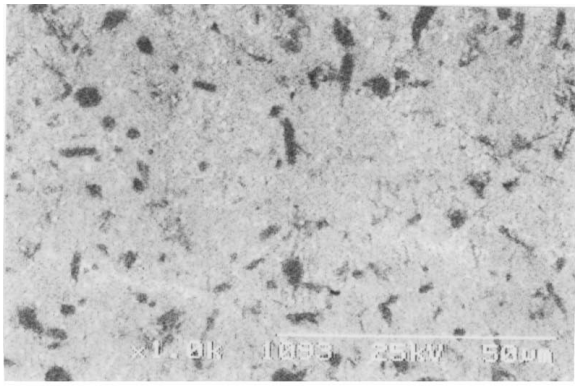

(a)

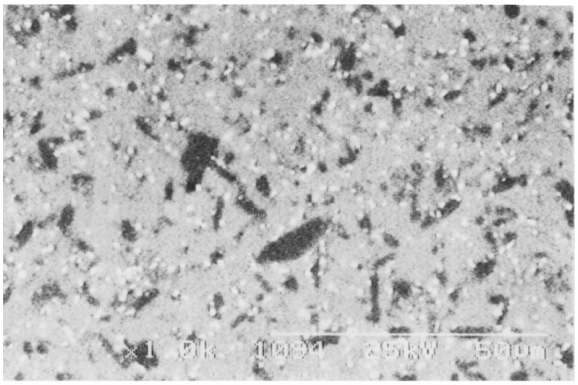

(b)

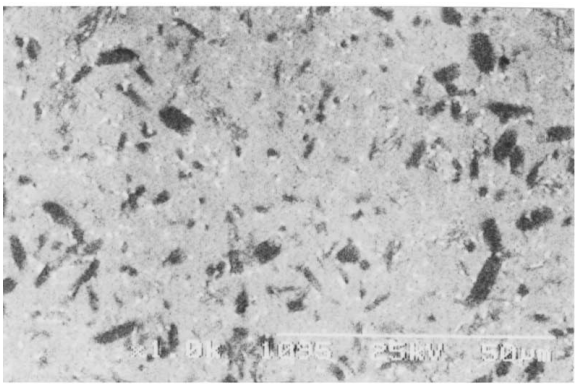

(c)

Figure 3 Backscattered SEM micrographs illustrating the microstructural changes in grain morphology and phase distribution in Yb-sialon before (a) and after heat-treatment (b) as well as resintering (c), in which β' grains are black, α' grains are grey and grain boundary phases are white.

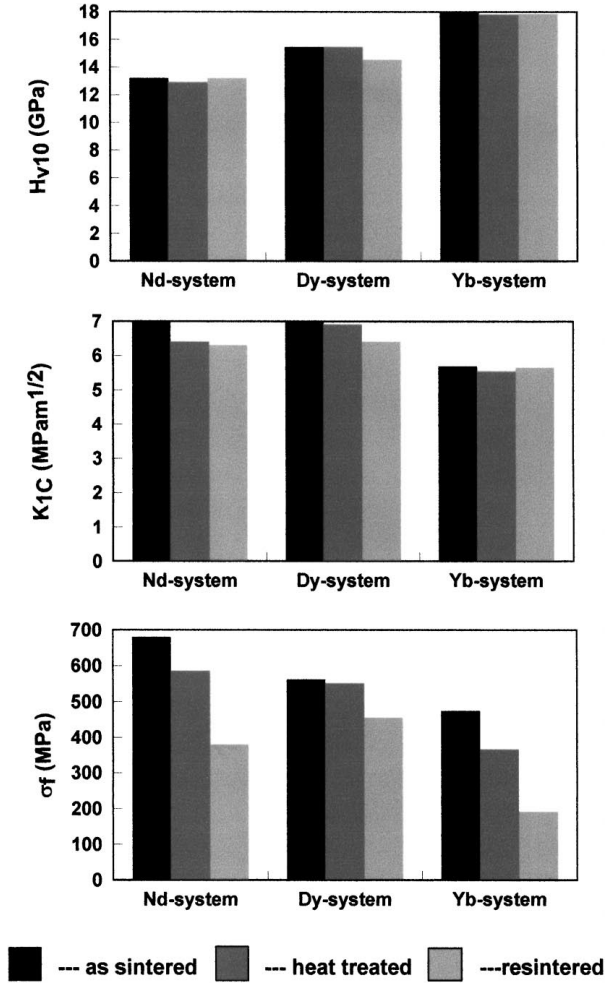

Figure 4 The values of Vickers hardness, indentation fracture toughness and flexural strength of Ln-sialons before and after post-heat-treatment.

providing considerable variation in mechanical properties of the final materials. Fig. 4 shows the measured Vickers hardness, indentation fracture toughness, and bending strength values at room temperature for the three kinds of materials, as-sintered, heat-treated and re-sintered. The maximum values of K_{1C} and σ_f were determined as 7.0 MPa $m^{1/2}$ and 680 MPa respectively for the Nd-samples, compared with the minimum of 5.6 MPa $m^{1/2}$ and 470 MPa for the Yb-samples. The main contribution for improving the K_{1C} and σ_f in Nd-samples is provided by elongated grain pull-out. The overall microstructural features are quite easily seen from SEM micrographs in the backscattered mode, which yield a pronounced contrast between the different phases as shown in Fig. 2. In Nd-densified samples, many more equiaxed α sialon grains transformed to β sialon with a higher proportion of elongated grains contributing to the enhanced toughness. Furthermore, the bonding between elongated grains and the matrix is weak enough to provide ideal structure to promote debonding/sliding, and hence the pull-out mechanism seen in Fig. 5. Fig. 5 indicates a rough fracture surface (a) of the Nd-samples after bend strength testing and (b) an image of crack propagation in the indented samples. These fracture characteristics were attributed to the debonding, crack deflection, crack bridging, and elongated grain pull-out mechanisms which were very effective in increasing the toughness [17]. The surprising thing was that the K_{1C} values were not improved significantly as a result of the heat-treatment; the values of K_{1C} before heat-treatment were higher due to the existing network of large elongated β' grains but even though the amount of β' increased after heat-treatment, the aspect ratio of elongated grains did not considerably increase beyond a certain value. Instead, grain growth occurred, influenced by both coalescence of grains and the increased liquid content released from the α' lattice during transformation. Fig. 2a–c illustrate the changes in β' grain morphology in a Nd-sialon sample before and after both heat-treatment and re-sintering; here the fiber-like, elongated grains are β' phase. One notable microstructural feature is that β' grains are thinner in as-sintered samples than in either of the post-heat-treated

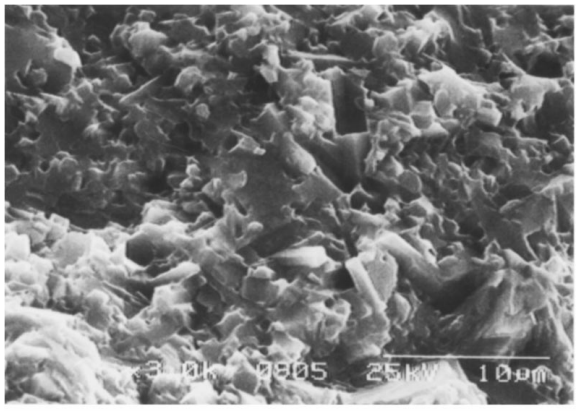

(a)

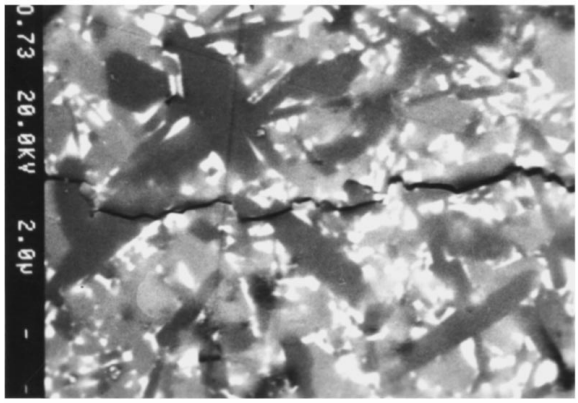

(b)

Figure 5 Secondary SEM micrograph (a) illustrating a rough fracture surface and backscattered SEM micrograph (b) showing the crack propagation in Nd-added samples indicating extensive debonding, crack deflection, crack bridge, and pull-out mechanisms.

two ones. After heat-treatment, β' grains grew and coalesced into larger, thicker ones, thus limiting the strength and toughness of the samples and leading to a decrease in σ_f and K_{1C}.

As discussed above, Dy_2O_3 and Yb_2O_3 were equally effective as densifying additives for sialons and more effective for stabilizing α' than Nd_2O_3. There is no doubt that Dy-sialon and Yb-sialon were harder because more equiaxed α' grains were present in the samples as illustrated in Fig. 3 for the Yb-samples. The highest value of hardness of 18.0 GPa was achieved as shown in Fig. 4. All re-sintered Ln-densified samples underwent $\beta \rightarrow \alpha$ transformation to some degree leading to a degradation of mechanical properties due to significant weight loss and pore formation.

4. Conclusions

(1) Dense rare earth Ln-sialons (Ln = Nd, Dy, and Yb) of overall composition $Ln_{0.33}Si_{9.3}Al_{2.7}O_{1.7}N_{14.3}$ were prepared by hot-pressing at 1800°C. A highest K_{1C} of 7.0 MPa $m^{1/2}$ and a highest σ_f of 680 MPa were obtained for Nd-sialon. But the Yb-sialon sample possessed the highest hardness of 18.0 GPa.

(2) Ln-sialons prepared in this way were further post-heat-treated at 1450°C for 96 h and 1800°C for 1 h. It was found that the additives (Nd_2O_3, Dy_2O_3, and Yb_2O_3) used for densification had significantly different effects on the thermal stability of α' phase allowing easy tailoring of microstructure and mechanical properties.

(3) Nd-α-sialon was unstable on post-heat-treatment. Much more α-sialon therefore transformed to β-sialon with Nd-melilite forming as the dominant grain boundary phase. The highest measured K_{1C} value was obtained in this system due to the elongated β-sialon grains formed in the matrix promoting debonding, crack deflection, crack bridging, and multiple pull-out mechanisms.

(4) Dy_2O_3 and Y_2O_3 were equally good as additives for densifying sialon ceramics and were more efficient in stabilizing the α-sialon structure during the post-heat-treatment. Consequently, Dy- and Yb-sialon possessed a higher hardness, because of the higher proportion of equiaxed α-sialon grains in the samples.

Acknowledgements

We thank the Royal Society of the United Kingdom, the State Key Lab of High Performance Ceramics and Superfine Microstructure, Shanghai Institute of Ceramics, and National Natural Science Foundation, China, for providing financial supports for this work.

References

1. T. EKSTRÖM and M. NYGREN, *J. Am. Ceram. Soc.* **75** (1992) 259.
2. S. T. BULJAN, J. G. BALDONI and M. L. HUCKABEE, *Am. Ceram. Soc. Bull.* **66** (1987) 347.
3. P. F. BECHER, *J. Am. Ceram. Soc.* **74** (1991) 255.
4. H. MANDAL and D. P. THOMPSON, *J. Mater. Sci. Lett.* **15** (1995) 1435.
5. C. GRESKOVICH and G. E. GAZZA, *J. Mat. Sci.* **4** (1985) 195.
6. D. P. THOMPSON, *Nature* **389** (1997) 675.
7. Y. B. CHEN and D. P. THOMPSON, *J. Eur. Ceram. Soc.* **14** (1994) 13.
8. L.-O. NORDBERG, Z. J. SHEN, T. EKSTRÖM and M. NYGREN, *ibid.* **17** (1995) 575.
9. H. MANDAL, D. P. THOMPSON and T. EKSTRÖM, *ibid.* **12** (1993) 421.
10. H. MANDAL, D. P. THOMPSON and T. EKSTRÖM, in "Materials for Advanced Technology Applications: Key Engineering Materials," edited by M. Buggy and S. Hampshire (Elsevier Applied Science, Switzerland, 1991) 187.
11. A. G. EVANS and A. CHARLES, *J. Am. Ceram. Soc.* **59** (1976) 371.
12. I-WEI CHEN and A. ROSENFLANZ, *Nature* **389** (1997) 701.
13. L.-O. NORDBERG, T. EKSTRÖM, G. SVENSSON and S. L. WEN, *J. Hard Mater.* **4** (1993) 121.
14. S. HAMPSHIRE, H. K. PARK, D. P. THOMPSON and K. H. JACK, *Nature* **274** (1978) 880.
15. H. MANDAL, D. P. THOMPSON, Q. LIU, L. GAO and D. S. YAN, *Eur. J. of Sol. State Inorg. Chem.* **34** (1997) 179.
16. H. MANDAL, N. CAMUSCU and D. P. THOMPSON, *J. Eur. Ceram. Soc.* **17** (1997) 599.
17. H. FUJITA, M. ENOKI and T. KISHI, *Mater. Trans. Jpn. Inst. Met.* **37** (1996) 769.

Received 10 March
and accepted 1 November 1999